

## PUBLISHED VERSION

Francois, Alexandre; Himmelhaus, Michael.

Optical biosensor based on whispering gallery mode excitations in clusters of microparticles, *Applied Physics Letters*, 2008; 92(14):www1-3.

© 2008 American Institute of Physics. This article may be downloaded for personal use only. Any other use requires prior permission of the author and the American Institute of Physics.

The following article appeared in *Appl. Phys. Lett.* **92**, 141107 (2008) and may be found at <http://link.aip.org/link/doi/10.1063/1.2907491>

### PERMISSIONS

[http://www.aip.org/pubservs/web\\_posting\\_guidelines.html](http://www.aip.org/pubservs/web_posting_guidelines.html)

The American Institute of Physics (AIP) grants to the author(s) of papers submitted to or published in one of the AIP journals or AIP Conference Proceedings the right to post and update the article on the Internet with the following specifications.

On the authors' and employers' webpages:

- There are no format restrictions; files prepared and/or formatted by AIP or its vendors (e.g., the PDF, PostScript, or HTML article files published in the online journals and proceedings) may be used for this purpose. If a fee is charged for any use, AIP permission must be obtained.
- An appropriate copyright notice must be included along with the full citation for the published paper and a Web link to AIP's official online version of the abstract.

31<sup>st</sup> March 2011

<http://hdl.handle.net/2440/55462>

## Optical biosensor based on whispering gallery mode excitations in clusters of microparticles

Alexandre Francois and Michael Himmelhaus<sup>a)</sup>

Bio-Nanotechnology Research Project, Research and Development Division, FUJIREBIO, Inc.,  
51 Komiya-cho, Hachioji-shi, Tokyo 192-0031, Japan

(Received 29 January 2008; accepted 18 March 2008; published online 8 April 2008)

A new concept for an optical biosensor based on whispering gallery mode (WGM) excitations in clusters of spherical microresonators is presented. Clusters of microresonators offer the advantage to exhibit specific WGM spectra that can be considered as their fingerprint. Therefore, individual clusters can be traced throughout an experiment even without knowledge of their precise positions. Polyelectrolyte adsorption onto clusters of 10  $\mu\text{m}$  polystyrene spheres is monitored *in situ*. It is shown that the WGMs shift to the same amount as those of a single microresonator and thus sensitivity does not depend on the number of microresonators present in the cluster. © 2008 American Institute of Physics. [DOI: 10.1063/1.2907491]

Microscopic optical resonators based on whispering gallery mode (WGM) excitation have attracted much attention due to their fascinating ability to confine light on the micron scale<sup>1</sup> and have found applications<sup>2</sup> as miniature laser sources,<sup>3–6</sup> optical waveguides,<sup>6</sup> filters,<sup>7</sup> and mechanical<sup>8</sup> or biological<sup>9,10</sup> sensors. WGMs are generated when light is trapped in a resonator by total internal reflection and propagates along its inner circumference. The simplest geometries for such systems are rings,<sup>11</sup> spheres,<sup>4</sup> and cylinders.<sup>12</sup> Corresponding modes can also be observed in nanocrystals with hexagonal cross section<sup>13</sup> or even in asymmetric optical cavities.<sup>14</sup> WGM can achieve extremely low losses<sup>1</sup> when the refractive index contrast at the resonator boundaries is high, the radius of curvature exceeds several wavelengths, and intrinsic scattering as well as surface roughness of the cavity are small.<sup>15</sup>

In fact, WGM positions are very sensitive to any modification of either the refractive index in vicinity of the resonator or shape and refractive index of the cavity.<sup>16</sup> This phenomenon has led to the development of various optical biosensors,<sup>9,10,17–19</sup> which achieve high sensitivity and can even provide information about the orientation of the absorbed molecules.<sup>20</sup> For the detection of biospecific interactions, the cavity surface can be accordingly surface functionalized.<sup>21</sup>

Due to their high  $Q$  factors,<sup>15</sup> so far most biosensors based on WGM have been made of single silica microspheres or toroids with a radius between 60 and 200  $\mu\text{m}$ .<sup>9,10,17–19</sup> In such case, WGM excitation is achieved by applying a narrow-band light source, such as a distributed feedback laser diode, and evanescent field coupling between the microsphere and a prism or an optical fiber. This detection scheme requires a very precise control of both the positioning of the microsphere with respect to the prism or optical fiber<sup>22</sup> and the frequency and intensity of the light source. Considering that typically many single resonators have to be measured either in order to increase the accuracy of the detection or for multiplexed detection in an array format, the task becomes complex, thereby limiting the prospects of such sensors.

In this letter, a new approach for optical biosensing is presented utilizing WGM excitations in clusters of fluorescent microspheres as the sensing element. The clusters consist of polystyrene (PS) microspheres (Polysciences, Inc., Warrington) with a higher refractive index ( $n_{\text{PS}}=1.59$ ) compared to silica ( $n_{\text{SiO}_2}=1.46$ ), which allows the reduction in the microsphere radius down to 5  $\mu\text{m}$  (standard deviation = 0.4  $\mu\text{m}$ ) without loss of the ability for WGM excitation even in an aqueous environment. The microspheres were doped with a fluorescent laser dye (Coumarin 6G) in order to excite WGM from the interior of the particle under exposure to a cw-HeCd laser operated at 442 nm. This kind of excitation supersedes the mechanical precision required for evanescent field coupling. The microspheres were randomly deposited on a thin glass slide by drop coating from highly diluted suspension in order to form clusters of various sizes; then, a microfluidic flow cell made from polydimethylsiloxane with a size of the flow channel of  $15 \times 2 \times 0.1 \text{ mm}^3$  was built around the sample. An inverted microscope (Nikon TS100) was used to collect the signal from a single microsphere or cluster. For acquisition of the WGM spectra, a high-resolution monochromator [Jobin Yvon TRIAX 550, 600 l/mm, 0.126 nm optical resolution with an entrance slit width of 40  $\mu\text{m}$  and the chosen charge coupled device (CCD)] and a cooled CCD camera (Andor Technology DU 440) were applied.

Polyelectrolytes (PEs) were chosen as a well-defined model system<sup>23</sup> to determine the sensitivity of clusters of microspheres with respect to the adsorption of organic molecules onto their surface. Poly(allylamine hydrochloride) (PAH) [molecular weight of (MW) 15.000 Da] and poly(sodium 4-styrenesulfonate) (PSS) (MW of 70.000 Da) (both Sigma Aldrich) were alternately deposited by means of the layer-by-layer technique described elsewhere.<sup>23,24</sup> WGM measurements were performed in Millipore water prior to and after each step of PAH/PSS bilayer deposition, which was repeated for several times to monitor the change in the WGM spectra as a function of increasing film thickness. The resulting WGM spectra for a single microsphere and a cluster composed of three microspheres are presented in Figs. 1(a) and 1(b), respectively. For the single microsphere, the periodic pattern of the first order TE and TM WGMs can be clearly seen because higher order mode exci-

<sup>a)</sup>Electronic mail: ml-himmelhaus@fujirebio.co.jp.

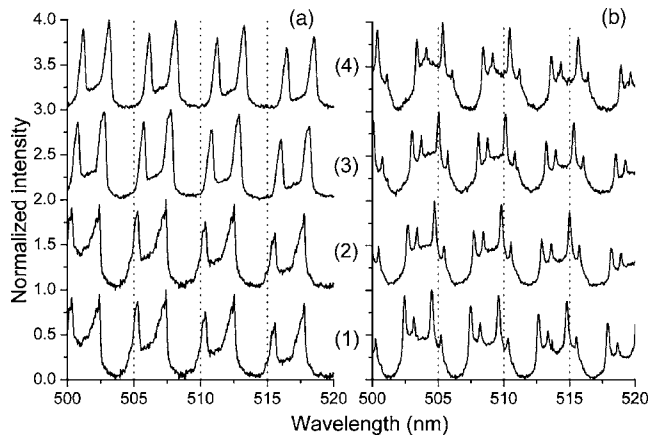


FIG. 1. WGM spectra of (a) a single microsphere and (b) a cluster of three microspheres, respectively, upon sequential deposition of several PAH/PSS bilayers: (1) WGM spectra before PE deposition, (2) after first bilayer, (3) after second bilayer, and (4) after third bilayer; Spectra were vertically displaced for clarity.

tations as they may be observed in the dry state<sup>25</sup> are quenched in water. The WGM wavelength shift toward higher wavelengths (for both TE and TM) upon deposition of the PE films can also be observed. For the cluster, the WGM spectra exhibit a more complex structure than those of the single sphere due to both the superposition of the first order TE and TM WGMs emitted by each individual microsphere constituting the cluster and additional modes that may arise from coupling between the microspheres.<sup>26–28</sup> Most importantly, upon deposition of PE onto the cluster, all peaks observable prior to the coating remain present with similar line

shape and are simply shifted toward higher wavelengths as a whole, in a similar fashion as those of the single microsphere. This is an important finding because in contrast to single microspheres, each cluster exhibits a characteristic WGM spectrum, which sensitively depends on its composition, i.e., on the number of microspheres within the cluster as well as their size<sup>28</sup> and their positioning<sup>27</sup> with respect to each other. Because of this strong dependence, a variety of clusters even with same particle number and same nominal size can be distinguished from each other, given that even the best commercially available monodisperse particle suspensions exhibit a size distribution of  $>3\%$ . For example, under the conditions used in the present study, i.e., a nominal bead radius of  $5\ \mu\text{m}$  and an optical resolution of the detection system of  $0.126\ \text{nm}$ , about 240 different bead sizes can be distinguished within a size range of  $\pm 3\%$ .<sup>29</sup> Accordingly,  $(240)^2/2! = 28\ 800$  dimers and  $(240)^3/3! = 2.3 \times 10^6$  trimers may be formed, which all exhibit different spectra, so that the probability of finding two clusters in the same sample exhibiting the same spectrum is basically negligible. Therefore, a cluster's characteristic WGM spectrum can be considered as a fingerprint, which allows its identification even in the presence of many others on the surface, thereby paving the way for multiple particle tracking and sensing in high density array formats.

To avoid tedious peak-by-peak fitting and thus to further facilitate array sensing, an autocorrelation function was used to determine the average WGM wavelength shift due to the adsorption of PE. The results of the autocorrelation between WGM spectra measured prior to the deposition of PE and

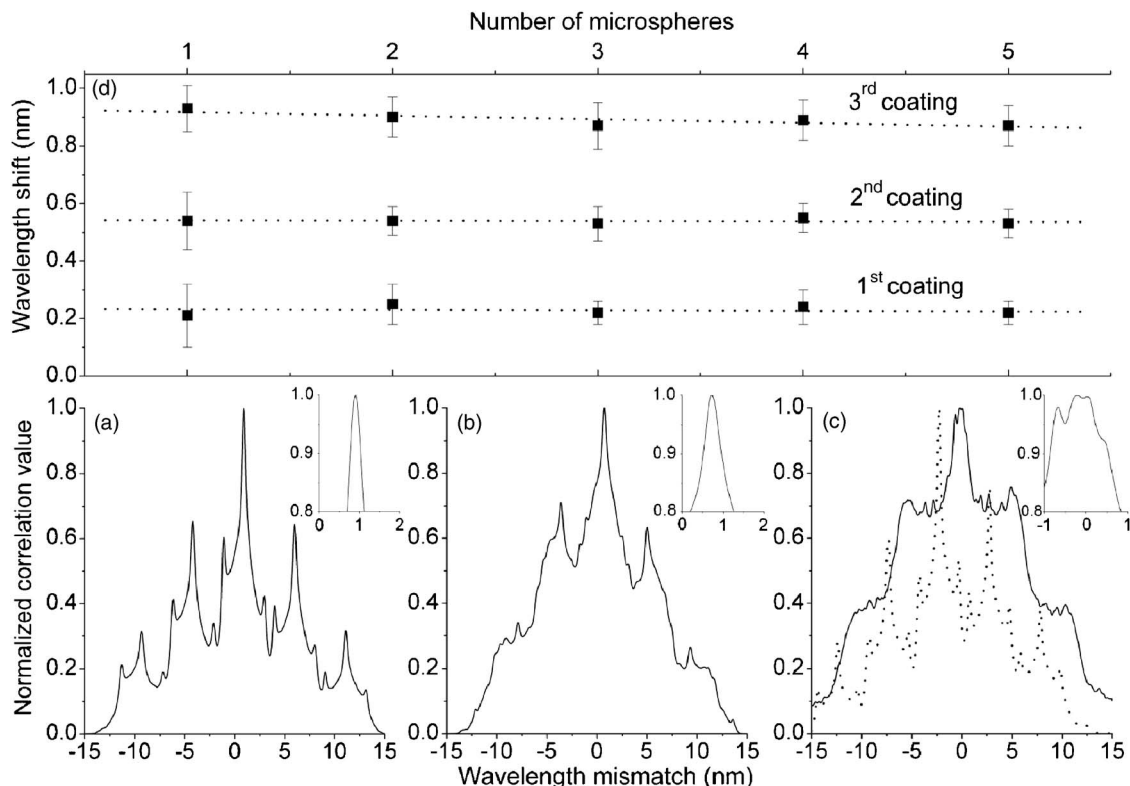


FIG. 2. Results of the autocorrelation between a first spectrum prior to coating and a second one taken after deposition of three PAH/PSS bilayers for (a) a single microsphere and (b) a cluster of three microspheres; (c) results of a correlation analysis of spectra obtained from two different single spheres (dotted line) as well as two different trimers (solid line), respectively, without PE coating. All correlations shown in (a)–(c) were calculated with a step width of  $0.039\ \text{nm}$  over a wavelength range of  $15\ \text{nm}$ ; (d) average WGM wavelength shift as a function of the number of microspheres present in the cluster for three different PE layer thicknesses. The errors shown are the standard deviations of the experimental errors calculated from 10 to 12 measurements on different beads or clusters for each data point.

after the third coating are shown in Figs. 2(a) and 2(b), respectively, for both a single microsphere and a cluster of three. In both graphs, the autocorrelation is represented by a symmetrical function with a Gaussian envelope, from which the average WGM wavelength shift induced by the three bilayers of PE can be immediately obtained by determination of the position of its absolute maximum [cf. the insets of Figs. 2(a) and 2(b)]. This also confirms the earlier observation that the deposition of PE mainly causes a peak shift but leaves the line shape of the spectra basically unaltered. Similar measurements were performed for various clusters with different sizes and configurations, and the results show that whatever the cluster size and shape may be, the WGM wavelength shift always resembles that of a single microsphere [Fig. 2(d)]. Therefore, optical sensing using WGM excitations in clusters of microspheres is as sensitive as when using single spheres with the additional advantage of the characteristic fingerprint, which is particularly interesting for simultaneous tracking of a variety of clusters and sensing in array formats. To validate the specificity of the fingerprint, cross correlations were calculated between spectra of different clusters or single microspheres, respectively. In fact, in that case, as shown in Fig. 2(c) for two clusters containing the same number of microspheres, the correlation has a much less pronounced maximum of much wider peak width [cf. the inset of Fig. 2(c)], thus allowing a clear distinction from the result of the autocorrelation, as shown in Fig. 2(b). On the other hand, as also shown in Fig. 2(c), when performing the same calculation on spectra of two different single microspheres, the correlation yields a similar result to that of an autocorrelation performed between two spectra from the same sphere [cf. Fig. 2(a)]. This implies that two different single microspheres cannot be distinguished from each other by means of a correlation analysis.

The observation that clusters are as sensitive as single microspheres means further that the mathematical description developed for sensing with single spheres can—at least in parts—also be applied to clusters. In the limit  $e \ll R$ , the thickness  $e$  of the deposited PE layer can be calculated from the WGM wavelength shift  $\delta\lambda$  by  $\delta\lambda/\lambda = \delta R/R = n_L e/n_S R$ ,<sup>25</sup> where  $\lambda$  is the position of the considered WGM peak,  $\delta R$  the effective increase in the microsphere radius  $R$  due to the deposition, and  $n_L = 1.47$  and  $n_S$  are the refractive indices of deposited layer and microsphere, respectively. Note that only the effective increase in sphere radius is accounted for by introducing the factor  $n_L/n_S$ . For  $\delta\lambda$ , the results of the autocorrelation spanning the range from 500 to 515 nm were used, so that  $\lambda$  was set to  $\lambda = 507.5$  nm in the calculation. We found the error introduced by this kind of averaging below the spectral resolution of our experimental setup and thus neglect it here. We obtained a thickness of  $e_1 = 2.5 \pm 0.76$  nm for the first bilayer,  $e_2 = 3.2 \pm 0.32$  nm for the second, and  $e_3 = 3.7 \pm 0.28$  nm for the third bilayer, respectively. In good agreement, the literature values for the thickness of PAH/PSS bilayers are about 3.4 nm on average.<sup>23,24</sup> It is known, however, that the first few layers form poorer films, which is corroborated by our findings.<sup>30</sup>

In conclusion, we have shown that clusters of microspheres can be used for optical *in situ* biosensing by means of WGM excitation. Each cluster exhibits a specific WGM spectrum that can be considered as its fingerprint and latter can be used for the identification of the traced cluster by means of a correlation function, which may simultaneously

yield the average WGM wavelength shift induced by the adsorption of a (bio)molecule onto the cluster's surface. The shifts found for clusters had the same magnitude as those observed under the same conditions with single microspheres. Therefore, for the calculation of the thickness of the deposited layer, a simple model derived for a single microsphere could be applied. This new detection scheme is particularly useful for the integration of a large number of detection sites within a single biosensor chip ensuring that each cluster can be readout properly even without knowledge of its precise position on the chip surface.

The authors would like to acknowledge Dr. S. Krishnamoorthy for valuable discussions.

- <sup>1</sup>A. B. Matsko and V. S. Ilchenko, *IEEE J. Sel. Top. Quantum Electron.* **12**, 3 (2006).
- <sup>2</sup>V. S. Ilchenko and A. B. Matsko, *IEEE J. Sel. Top. Quantum Electron.* **12**, 15 (2006).
- <sup>3</sup>J. L. Jewell, S. L. McCall, Y. H. Lee, A. Scherer, A. C. Gossard, and J. H. English, *Appl. Phys. Lett.* **54**, 1400 (1989).
- <sup>4</sup>M. Kuwata-Gonokami, K. Takeda, H. Yasuda, and K. Ema, *Jpn. J. Appl. Phys., Part 2* **31**, L99 (1992).
- <sup>5</sup>S. M. Spillane, T. J. Kippenberg, and K. J. Vahala, *Nature (London)* **415**, 621 (2002).
- <sup>6</sup>V. N. Astratov, J. P. Franchak, and S. P. Ashili, *Appl. Phys. Lett.* **85**, 5508 (2004).
- <sup>7</sup>L. Maleki, A. A. Savchenko, A. B. Matsko, and V. S. Ilchenko, *Proc. SPIE* **5435**, 178 (2004).
- <sup>8</sup>M. Gerlach, Y. P. Rakovich, and J. F. Donegan, *Opt. Express* **15**, 3597 (2007).
- <sup>9</sup>V. S. Ilchenko and L. Maleki, *Proc. SPIE* **4270**, 120 (2001).
- <sup>10</sup>F. Vollmer, D. Braun, A. Libchaber, M. Khoshima, I. Teraoka, and S. Arnold, *Appl. Phys. Lett.* **80**, 4057 (2002).
- <sup>11</sup>D. K. Armani, T. J. Kippenberg, S. M. Spillane, and K. J. Vahala, *Nature (London)* **421**, 925 (2003).
- <sup>12</sup>H. J. Moon, G. W. Park, S. B. Lee, K. An, and J. H. Lee, *Opt. Commun.* **235**, 401 (2004).
- <sup>13</sup>T. Nobis, E. M. Kaidashev, A. Rahm, M. Lorenz, and M. Grundmann, *Phys. Rev. Lett.* **93**, 103903 (2004).
- <sup>14</sup>J. U. Nöckel and A. D. Stone, *Nature (London)* **385**, 45 (1997).
- <sup>15</sup>M. L. Gorodetsky, A. A. Savchenko, and V. S. Ilchenko, *Opt. Lett.* **21**, 453 (1996).
- <sup>16</sup>G. Schweiger and M. Horn, *J. Opt. Soc. Am. B* **23**, 212 (2006).
- <sup>17</sup>A. Serpengüzel, S. Isci, T. Bilici, and A. Kurt, *Proc. SPIE* **5317**, 180 (2004).
- <sup>18</sup>I. M. White, N. M. Hanumegowda, and X. Fan, *Opt. Lett.* **30**, 3189 (2005).
- <sup>19</sup>A. M. Armani, R. P. Kulkarni, S. E. Fraser, R. C. Flagan, and K. J. Vahala, *Science* **317**, 783 (2007).
- <sup>20</sup>M. Noto, D. Keng, I. Teraoka, and S. Arnold, *Biophys. J.* **92**, 4466 (2007).
- <sup>21</sup>F. Vollmer, S. Arnold, D. Braun, I. Teraoka, and A. Libchaber, *Biophys. J.* **85**, 1974 (2003).
- <sup>22</sup>Z. Guo, H. Quan, and S. Pau, *J. Phys. D* **39**, 5133 (2006).
- <sup>23</sup>G. Decher, *Science* **277**, 1232 (1997).
- <sup>24</sup>M. Lösche, J. Schmitt, G. Decher, W. G. Bouwman, and K. Kjaer, *Macromolecules* **31**, 8893 (1998).
- <sup>25</sup>A. Weller, F. C. Liu, R. Dahint, and M. Himmelhaus, *Appl. Phys. B: Lasers Opt.* **90**, 561 (2008).
- <sup>26</sup>Y. P. Rakovich, J. F. Donegan, M. Gerlach, A. L. Bradley, T. M. Connolly, J. J. Boland, N. Gaponik, and A. Rogach, *Phys. Rev. A* **70**, 051801 (2004).
- <sup>27</sup>S. P. Ashili, V. N. Astratov, and E. C. H. Sykes, *Opt. Express* **14**, 9460 (2006).
- <sup>28</sup>T. Mukaiyama, K. Takeda, H. Miyazaki, Y. Jimba, and M. Kuwata-Gonokami, *Phys. Rev. Lett.* **82**, 4623 (1999).
- <sup>29</sup>With an optical resolution of  $\Delta\lambda = 0.126$  nm and  $R = 5$   $\mu\text{m}$ , the minimum detectable change in the bead radius amounts to  $\Delta R = R \times \Delta\lambda/\lambda = 1.26$  nm and thus to  $2.5 \times 10^{-2}\%$  of the nominal bead radius at  $\lambda = 500$  nm. Within a  $\pm 3\%$  size distribution, this results in  $6\%/2.5 \times 10^{-2}\% = 238$  experimentally distinguishable bead sizes.
- <sup>30</sup>J. Schmitt, T. Grünwald, G. Decher, P. S. Pershan, K. Kjaer, and M. Lösche, *Macromolecules* **26**, 7058 (1993).